

Relationship Between Conformational Flexibility and Chelate Cooperativity

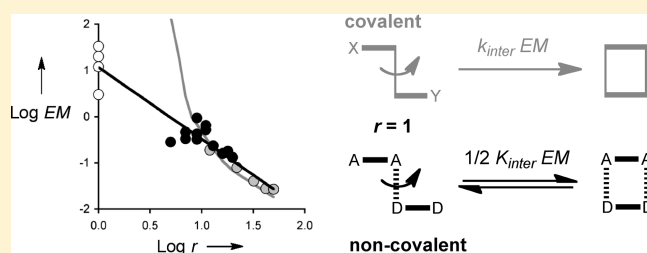
M. Cristina Misuraca,[†] Tudor Grecu,[†] Zoraida Freixa,[‡] Valentina Garavini,[†] Christopher A. Hunter,^{*,†} Piet W.N.M. van Leeuwen,[‡] M. Dolores Segarra-Maset,[‡] and Simon M. Turega[†]

[†]Department of Chemistry, University of Sheffield, Sheffield S3 7HF, United Kingdom

[‡]Institute of Chemical Research of Catalonia (ICIQ), Av. Països Catalans 16, 43007 Tarragona, Spain

S Supporting Information

ABSTRACT: A family of four biscarbamates (AA) and four bisphenols (DD) were synthesized, and H-bonding interactions between all AA•DD combinations were characterized using ¹H NMR titrations in carbon tetrachloride. A chemical double mutant cycle analysis shows that there are no secondary electrostatic interactions or allosteric cooperativity in these systems, and the system therefore provides an ideal platform for investigating the relationship between chemical structure and chelate cooperativity. Effective molarities (EMs) were measured for 12 different systems, where the number of rotors in the chains connecting the two H-bond sites was varied from 5 to 20. The association constants vary by less than an order of magnitude for all 12 complexes, and the variation in EM is remarkably small (0.1–0.9 M). The results provide a relationship between EM and the number of rotors in the connecting chains (r): $EM \approx 10r^{-3/2}$. The value of 10 M is the upper limit for the value of EM for a noncovalent intramolecular interaction. Introduction of rotors reduces the value of EM from this maximum in accord with a random walk analysis of the encounter probability of the chain ends ($r^{-3/2}$). Noncovalent EMs never reach the very high values observed for covalent processes, which places limitations on the magnitudes of the effects that one is likely to achieve through the use of chelate cooperativity in supramolecular assembly and catalysis. On the other hand, the decrease in EM due to the introduction of conformational flexibility is less dramatic than one might expect based on the behavior of covalent systems, which limits the losses in binding affinity caused by poor preorganization of the interaction sites.



INTRODUCTION

Cooperativity is a central concept in supramolecular science. Systems that feature multiple noncovalent interactions show significant increases in thermodynamic and kinetic stability compared with the corresponding single point interactions.^{1–6} Although two different forms of cooperativity have been identified, allosteric and chelate,^{7,8} it is chelate cooperativity (or multivalency) that is usually responsible for the all-or-nothing behavior that characterizes biological processes like folding and self-assembly.^{9–12} Chelate cooperativity is straightforward to implement in synthetic supramolecular design, and the multivalent approach to noncovalent chemistry is therefore beginning to find applications in nanotechnology.^{13–16} However, the quantitative relationship between chemical structure, supramolecular architecture, and noncovalent cooperativity remains largely unexplored.^{17–21} Although cooperative phenomena are widespread in biology, the complexity of these systems makes it difficult to dissect individual contributions to the overall behavior of the system. Synthetic supramolecular complexes, where structure and complexity can be controlled through synthesis, provide the ideal model systems for establishing quantitative structure–activity relationships,²² and here we use this approach to investigate chelate cooperativity.⁸

There are good methods available for estimating the properties of a single point H-bond interaction,^{23,24} but when there are multiple intermolecular contacts, communication between the coupled binding sites makes prediction problematic.^{25–31} The parameter which is used to quantify the chelate cooperativity associated with the formation of an intramolecular interaction is the product KEM , where K is the association constant for the corresponding intermolecular binding interaction under the same conditions, and EM is the effective molarity.⁸ When $KEM \gg 1$, the intramolecular process is strongly favored, and efficient assembly of the complex will take place. For relatively rigid complexes with good geometric complementarity, where there are no complications due to changes in conformational flexibility or conformational strain, the values of EM are on the order 10 M.^{24,32} For synthetic supramolecular systems that have been designed using high affinity binding sites and highly preorganized scaffolds, KEM is usually much greater than 1, and intramolecular interactions are therefore formed quantitatively. Under these conditions, the free energy of binding is an

Received: January 13, 2011

Published: March 18, 2011

additive function of the individual intermolecular contacts.^{32–34} When $KEM \approx 1$, there are mixtures of partially bound states, as well as the fully assembled complex, and the behavior of the system may be strongly dependent on small changes in conditions. This regime is common in biology but has been less widely investigated in synthetic model systems. When $KEM \ll 1$, there are no intramolecular interactions and no assembly of the desired complex.

The relationship between chemical structure and EM has been thoroughly explored for both the kinetics and the thermodynamics of covalent cyclization reactions: EM decreases with an increase in the conformational flexibility of the chain linking the reactive end groups and the degree of conformational strain introduced on cyclization.^{35,36} The thermodynamic consequences of freezing a single rotor at room temperature have been estimated at 5.6 kJ mol^{-1} for formation of a covalent bond, and this is borne out by the experimental data for cyclization of small rings.³⁷ However, as the ring size increases, the incremental effect of introducing additional rotors on EM decreases, due to the increased conformational mobility of the cyclic product.³⁵ In the limit of very large rings and very flexible molecules (polymers), the probability that an intramolecular reaction will take place between the two chain ends is found to vary as $N^{-3/2}$, where N is the number of bonds in the chain.³⁸ For noncovalent interactions, there is less experimental data available. Estimates of the thermodynamic cost of freezing a rotor by formation of a noncovalent interaction range from 0.5 to 5 kJ mol^{-1} .^{39–44} Whitesides studied the intramolecular binding of a protein to a ligand, where the two binding sites were connected via a flexible linker, and found a rather weak dependence of EM on linker length.²¹ Reinhoudt obtained a similar result using theoretical methods to estimate EM.¹⁷ Thus, it appears that noncovalent EMs are insensitive to conformational flexibility. In this paper, we quantify the effect of conformational flexibility on chelate cooperativity by measuring noncovalent EMs using a synthetic supramolecular model system.

■ APPROACH

We have shown previously that the phenol–carbamate interaction is ideally suited to construction of simple model systems for the quantification of cooperativity in H-bonded complexes.³¹ Phenol is a poor H-bond acceptor ($\beta = 2.7$) and one of the strongest H-bond donor functional groups ($\alpha = 3.8$). Carbamate is a poor H-bond donor ($\alpha = 2.4$) and a good H-bond acceptor ($\beta = 7.3$).²⁴ Thus, the phenol–phenol and the carbamate–carbamate interaction are both too weak to occur to any significant extent even in very nonpolar solvents, and the single point phenol–carbamate H-bonding interaction is sufficiently strong to allow accurate measurement of the 1:1 association constant in nonpolar solvents like carbon tetrachloride (K_{ref}). This provides a measurable noncooperative reference point that can be compared with cooperative interactions in systems that feature more than one H-bond. Here, we will examine the properties of complexes that make two phenol–carbamate H-bonds (Figure 1). By choosing the **AA•DD** motif, i.e., the 1:1 complex formed between a bisphenol and a biscarbamate, it is possible to avoid the potential problems of intramolecular folding and aggregation that are common in multiply H-bonded motifs.^{19,45} The use of relatively long linkers will ensure that the H-bonding sites in these systems are sufficiently far apart to minimize secondary

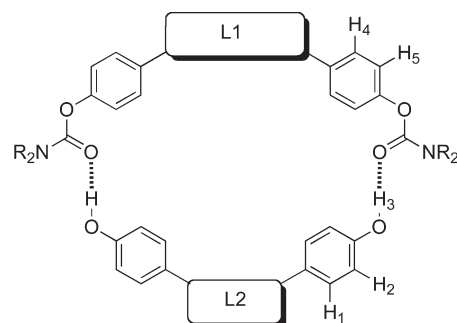


Figure 1. **AA•DD** complexes used to quantify the relationship between the chemical structures of the linkers, L1 and L2, and chelate cooperativity in formation of the intramolecular H-bond. The proton labeling scheme is shown (R = 2-ethylhexyl).

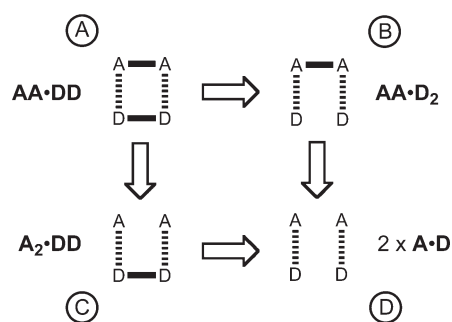


Figure 2. Chemical double mutant cycle used to assess the chelate cooperativity associated with the intramolecular H-bond in the doubly H-bonded **AA•DD** complex, state A.

electrostatic interactions and allosteric cooperativity, which usually complicates the analysis of multiply H-bonded complexes.⁴⁶ By synthesizing families of **AA** and **DD** compounds, it is possible to measure the stabilities of all pairwise **AA•DD** combinations, and hence quantify the relationship between chelate cooperativity and the nature of the linker. In this paper, we vary both the geometric complementarity and conformational flexibility of the linkers L1 and L2 in Figure 1 and quantify the effects on the effective molarity (EM) for the intramolecular H-bond interaction.

The free energy contribution of the intramolecular H-bond to the stability of the **AA•DD** complex can be evaluated using a chemical double mutant cycle (Figure 2).^{22,31} This requires the measurement of four different association constants, using the monofunctional reference compounds (**A** and **D**) and the bifunctional compounds (**AA** and **DD**). The double mutant cycle allows the quantification of any substituent effect, due to the presence of the linkers in the bifunctional compounds, as well as any allosteric cooperativity, due to complexation-induced changes in the intrinsic properties of the binding sites. Thus, the magnitude of the chelate cooperativity can be dissected from the other factors that contribute to the overall stability of the **AA•DD** complex. Equation 1 shows how the EM associated with the intramolecularity of the second H-bond is determined from the double mutant cycle experiment (the statistical factor of 2 accounts for the degeneracy of the symmetric **AA•DD** complex).

$$2EM = \frac{K_A K_D}{K_B K_C} = \frac{K(\text{AA}\cdot\text{DD})K^2(\text{A}\cdot\text{D})}{K(\text{AA}\cdot\text{D}_2)K(\text{A}_2\cdot\text{DD})} \quad (1)$$

RESULTS

Synthesis. We prepared a set of four bisphenols and four biscarbamates connected by linkers of varying length and flexibility (Scheme 1). Bisphenol **3a** is commercially available. Bisphenols **3b–d** were prepared from dihaloalkanes and the monoprotected bisphenol **1b**, followed by removal of the benzyl group by hydrogenation. The bisphenols were converted to the corresponding biscarbamates **4a–d** in one step. The monofunctional phenols **1a** and **1b** are commercially available. These were converted to the corresponding carbamates **2a** and **2b** to provide four reference compounds for studying singly H-bonded complexes (Scheme 1).

¹H NMR Dilution Experiments. Self-association of the compounds was investigated using ¹H NMR dilution experiments in carbon tetrachloride. The phenols are significantly less soluble than the carbamates, which are equipped with solubilizing groups. The solubility of phenol **3d** was too low even for use as a host in titration experiments, and will not be discussed further. No changes in chemical shift were observed for the phenols (0.1–0.6 mM) or for the carbamates (40–400 mM) in dilution experiments. Thus, self-association does not complicate the titration experiments. Table 1 lists the ¹H NMR chemical shifts of the phenols (**1** and **3**) and the carbamates (**2** and **4**) in carbon tetrachloride solution. The bifunctional compounds (**3** and **4**) have similar chemical shifts to the corresponding monofunctional reference compounds (**1** and **2**, respectively), which implies that there are no intramolecular H-bonds or aromatic interactions in the free state; i.e., the molecules adopt extended rather than folded conformations.

¹H NMR Titration Experiments. Complexation between the phenols and carbamates was investigated by ¹H NMR titration experiments in carbon tetrachloride. The titration data for the reference **A•D** complexes all fit well to a 1:1 binding isotherm. The association constants and limiting complexation-induced changes in chemical shift ($\Delta\delta$) are summarized in Table 2. The titration data for the reference complexes **A₂•DD** and **AA•D₂** fit well to 2:1 and 1:2 binding isotherms with identical stepwise microscopic association constants (Table 2). The phenol $\Delta\delta$

Table 1. ¹H NMR Chemical Shifts (ppm) Measured in CCl₄ at 298 K^a

	H ₁	H ₂	H ₃	H ₄	H ₅
1a	7.0	6.7	4.4		
1b	6.8	6.7	4.1		
3a	7.0	6.7	4.3		
3b	6.9	6.8	4.2		
3c	6.8	6.8	4.1		
2a				7.1	7.0
2b				7.0	6.9
4a				7.2	7.0
4b				7.1	7.0
4c				7.0	6.9
4d				6.9	6.8

^a See Figure 1 for the proton labeling scheme.

Scheme 1

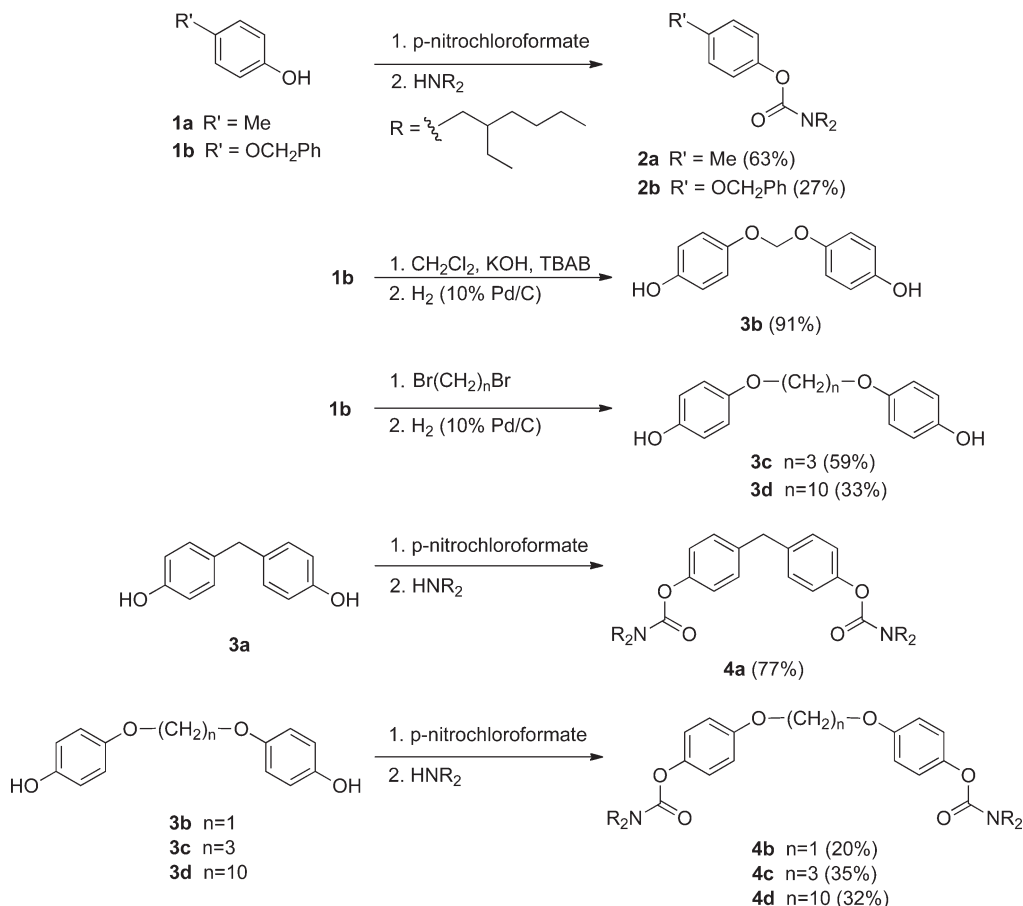


Table 2. Association Constants and Limiting Complexation-Induced Changes in Chemical Shift (ppm) for Formation of 1:1 and 2:1 Reference Complexes Determined from ^1H NMR Titrations at 298 K in CCl_4 ^a

complex	microscopic		macroscopic K_{obs}	$\Delta\delta$ (ppm)		
	K_2 (M^{-1})	K_1 (M^{-1})		H_1	H_2	H_3
D•A 1a•2a	17		17 M^{-1}	-0.2	-0.3	2.6
D•A 1a•2b	17		17 M^{-1}	-0.2	-0.3	2.6
D•A 1b•2a	19		19 M^{-1}	-0.2	-0.3	2.7
D•A 1b•2b	21		21 M^{-1}	-0.2	-0.3	2.6
D•AA 1b•4b	20		39 M^{-1}	-0.2	-0.3	2.7
D₂•AA (1b) ₂ •4b		20	380 M^{-2}	-0.2	-0.3	2.7
DD•A 3b•2b	20		41 M^{-1}	-0.1	-0.2	1.0 ^b
DD•A₂ 3b•(2b) ₂		20	420 M^{-2}	-0.2	-0.4	2.1

^a See Figure 1 for the proton labeling scheme. ^b Only one of the two OH groups is H-bonded in this 1:1 complex, and so this value is the average of a free and a bound OH chemical shift, i.e., $1/2(0.0 + 2.0)$ ppm. The same is true for the aromatic protons, H_1 and H_2 .

values are similar in all cases: small negative changes are observed for the CH protons, and large positive changes (+2–3 ppm) are observed for the OH protons. These changes in chemical shift are classic signatures of H-bonding interactions with the OH groups, and the fact that the values are similar for the $\text{A}_2\bullet\text{DD}$ and $\text{AA}\bullet\text{D}_2$ complexes indicates that both H-bonds are made in these complexes. The microscopic association constants for all of the complexes involving the monofunctional reference compounds are very similar ($K_{\text{ref}} = 17\text{--}21 \text{ M}^{-1}$). This result shows that the linkers have no significant effect on the intrinsic binding properties of the recognition units; i.e., there are no substituent effects on the H-bond properties of the phenol or carbamate. In addition, the observation of identical microscopic stepwise association constants for the $\text{A}_2\bullet\text{DD}$ and $\text{AA}\bullet\text{D}_2$ complexes implies that allosteric cooperativity is negligible. Thus, the data in Table 2 imply that K_{ref} is constant for these systems, i.e. $K_{\text{B}} = K_{\text{C}} = K_{\text{D}} = K_{\text{ref}}^2$, which greatly simplifies the double mutant cycle analysis in Figure 2. Under these conditions, $K(\text{AA}\bullet\text{DD}) = 2K_{\text{ref}}^2\text{EM}$.

The $\text{AA}\bullet\text{DD}$ titrations are potentially more complicated, because a number of different complexes are possible (Figure 3).⁸ The titrations were carried out under conditions where the guest (AA) was always present in a large excess, and the concentration of host (DD) was low ($[\text{DD}] \ll 1/K_{\text{ref}}$). This ensures that open oligomeric complexes, $o\text{-(AA)}_N\bullet(\text{DD})_N$, are not significantly populated, and higher order cyclic oligomers, $c\text{-(AA)}_N\bullet(\text{DD})_N$, are unlikely to be populated. Thus, three different complexes should be considered in the analysis of the titration data: the singly H-bonded 1:1 complex $o\text{-AA}\bullet\text{DD}$, the doubly H-bonded 1:1 complex $c\text{-AA}\bullet\text{DD}$, and the 2:1 complex $(\text{AA})_2\bullet\text{DD}$. The key parameter that determines speciation in this system is $1/2K_{\text{ref}}\text{EM}$, the dimensionless equilibrium constant between the open and closed 1:1 complexes. If $1/2K_{\text{ref}}\text{EM}$ is sufficiently large, then closed complex $c\text{-AA}\bullet\text{DD}$ will predominate, and a simple 1:1 binding isotherm will result.

The titration data for the $\text{AA}\bullet\text{DD}$ complexes fit well to a simple 1:1 binding isotherm in all cases, and the apparent association constant, K_1 , is an order of magnitude larger than the values of K_{ref} in Table 2. This suggests cooperative formation

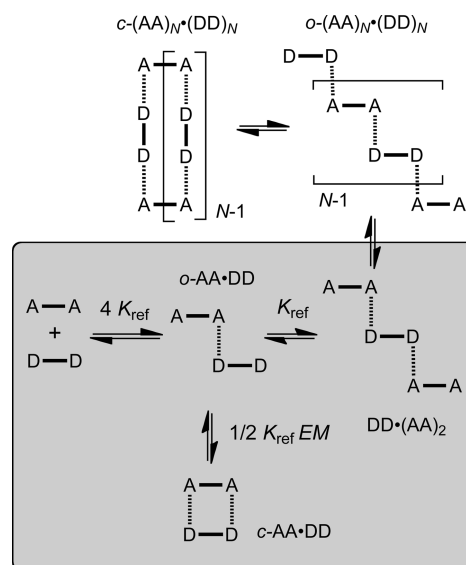


Figure 3. Various complexes are possible for the interaction of a bifunctional host (DD) with a bifunctional guest (AA). Under the conditions used, $[\text{DD}] \ll [\text{AA}]$ and $[\text{DD}] \ll 1/K_{\text{ref}}$, only the species in the box are significantly populated. K_{ref} is the 1:1 association constant for a complex featuring a single point phenol–carbamate H-bond. EM is the effective molarity for the intramolecular interaction. The statistical factors of 4 and $1/2$ account for the degeneracies of the complexes.

Table 3. Association Constants and Limiting Complexation-Induced Changes in Chemical Shifts (ppm) Obtained by Fitting the Data from ^1H NMR Titrations in CCl_4 at 298 K to a 1:1 Binding Isotherm^a

complex	K_1 (M^{-1})	$\Delta\delta$ (ppm)		
		H_1	H_2	H_3
3a•4a	200 ± 60	-0.2	-0.3	2.2
3a•4b	260 ± 130	-0.2	-0.4	2.2
3a•4c	290 ± 70	-0.2	-0.4	2.3
3a•4d	140 ± 30	-0.2	-0.3	2.3
3b•4a	320 ± 30	-0.2	-0.4	2.3
3b•4b	890 ± 260	-0.2	-0.5	2.4
3b•4c	630 ± 350	-0.2	-0.4	2.3
3b•4d	210 ± 10	-0.2	-0.3	2.3
3c•4a	280 ± 50	-0.2	-0.4	3.1
3c•4b	560 ± 80	-0.3	-0.5	2.3
3c•4c	280 ± 110	-0.2	-0.4	2.3
3c•4d	170 ± 10	-0.2	-0.4	2.3

^a See Figure 1 for proton labeling scheme. All experiments were repeated at least twice, and the average values are reported with errors at the 95% confidence limit.

of the doubly H-bonded 1:1 complex $c\text{-AA}\bullet\text{DD}$ in all cases. The limiting complexation-induced changes in chemical shifts ($\Delta\delta$) provide further evidence for the structures of the complexes (Table 3). The signals due to the bisphenol OH protons (H_3) show large positive changes in chemical shift (+2–3 ppm) that are characteristic of H-bonding interactions, and comparison with the corresponding $\Delta\delta$ values for the reference complexes suggests that both OH groups are fully H-bonded in the 1:1

Table 4. Association Constants and Complexation-Induced Changes in Chemical Shifts (ppm) Obtained by Fitting the Data from ^1H NMR Titrations in CCl_4 at 298 K to a 2:1 Binding Isotherm^a

complex	K_1 (M^{-1})	K_2 (M^{-2})	$\Delta\delta_1$ (ppm)			$\Delta\delta_2$ (ppm)		
			H ₁	H ₂	H ₃	H ₁	H ₂	H ₃
3a•4a	230 ± 70	1200	-0.2	-0.3	2.1	-0.2	-0.3	2.6
3a•4b	260 ± 80	1200	-0.1	-0.4	2.0	-0.3	-0.2	3.0
3a•4c	310 ± 30	1200	-0.2	-0.4	2.2	-0.3	-0.3	2.8
3a•4d	160 ± 10	1200	-0.2	-0.3	2.0	-0.2	-0.3	2.6
3b•4a	410 ± 40	1400	-0.2	-0.4	2.1	-0.2	-0.3	3.2
3b•4b	910 ± 310	1700	-0.2	-0.5	2.4	0.0	-0.2	2.7
3b•4c	650 ± 340	1700	-0.2	-0.4	2.3	-0.1	-0.2	2.6
3b•4d	240 ± 20	1700	-0.2	-0.3	2.1	-0.2	-0.3	2.8
3c•4a	310 ± 90	1400	-0.2	-0.4	2.7	-0.2	-0.3	3.5
3c•4b	540 ± 50	1700	-0.3	-0.5	2.3	0.1	-0.2	2.3
3c•4c	290 ± 90	1700	-0.2	-0.4	2.2	-0.1	-0.2	2.4
3c•4d	200 ± 10	1700	-0.4	-0.2	2.1	-0.3	-0.2	2.5

^a See Figure 1 for proton labeling scheme. K_1 and K_2 are the macroscopic association constants. The value of K_2 was fixed at $4K_{\text{ref}}^2$ using the values in Table 2. $\Delta\delta_1$ and $\Delta\delta_2$ are the limiting complexation-induced changes in chemical shift for the 1:1 and the 2:1 complexes, respectively.

complexes. The values of $\Delta\delta$ for the phenol CH protons (H₁ and H₂) are also very similar to those observed for the reference complexes, indicating that the recognition units are in similar environments in all cases.

Although there is no clear evidence for the presence of the *o*-AA•DD or (AA)₂•DD complexes in the titration data presented above, the speciation of these additional complexes can be estimated based on the value of K_{ref} .

$$K(o\text{-AA}\bullet\text{DD}) = 4K_{\text{ref}} \quad (2)$$

$$K[(\text{AA})_2\bullet\text{DD}] = 4K_{\text{ref}}^2 \quad (3)$$

Using these relationships, it is possible to refit the titration data to a 2:1 binding isotherm that allows for the presence of all three complexes.

$$K_1 = K(c\text{-AA}\bullet\text{DD}) + K(o\text{-AA}\bullet\text{DD}) \\ = 2K_{\text{ref}}^2\text{EM} + 4K_{\text{ref}} \quad (4)$$

$$K_2 = K[(\text{AA})_2\bullet\text{DD}] = 4K_{\text{ref}}^2 \quad (5)$$

When the data were reanalyzed using a 2:1 isotherm, the quality of the fit to the experimental data improved in every case. It is important to note that the value of K_1 was fitted as a variable in this analysis, but the value of K_2 was not: K_2 was fixed using eq 5 and the value of K_{ref} from Table 2. However, the limiting changes in chemical shift for the 1:1 and 2:1 species, $\Delta\delta_1$ and $\Delta\delta_2$, were fit as independent variables, because the value of $\Delta\delta_1$ depends on the relative populations of the open and closed 1:1 complexes. Thus, fitting to the 2:1 isotherm requires an extra variable compared with fitting to a 1:1 isotherm, and the quality of the fit to the experimental data is expected to improve automatically. Nevertheless, the root-mean-square difference between the calculated and experimental chemical shifts changed

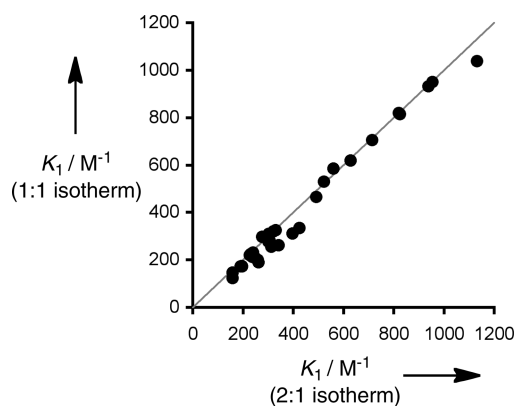


Figure 4. Association constant, K_1 , obtained by fitting the titration data to a 1:1 binding isotherm compared with the value of K_1 obtained by fitting the data to a 2:1 binding isotherm.

by as much as a factor of 10 in some titrations, indicating a significantly better fit to the 2:1 isotherm. Analysis of the speciation indicates that the population of the 2:1 complex does not exceed 30% in any of the titrations, and this has a small but detectable impact on the shape of the binding isotherm. Table 4 gives the association constants K_1 and the limiting complexation-induced changes in chemical shift obtained by fitting the titration data to a 2:1 binding isotherm. The values of K_1 reported in Table 4 are similar to those listed in Table 3 for the simple 1:1 isotherm (Figure 4).

The values of K_1 from the 2:1 binding isotherm were used in eq 6 to determine the values of EM and hence estimate the populations of the open and closed 1:1 complexes, *o*-AA•DD and *c*-AA•DD (eqs 7and8). The results are listed in Table 5.

$$\text{EM} = (K_1 - 4K_{\text{ref}})/2K_{\text{ref}}^2 \quad (6)$$

$$\text{population of } o\text{-AA}\bullet\text{DD} = 4K_{\text{ref}}/K_1 \quad (7)$$

$$\text{population of } c\text{-AA}\bullet\text{DD} = (K_1 - 4K_{\text{ref}})/K_1 \quad (8)$$

In all cases, the value of $1/2K_{\text{ref}}\text{EM}$ is greater than 1 (Table 5), which means that the closed complex, *c*-AA•DD, is more stable than the open partially bound 1:1 complex, *o*-AA•DD. However, the population of the partially bound open complex is significant. In the complex with the highest EM (3b•4b), 9% of the 1:1 complex is in the partially bound open form, but when the linker groups are long and flexible (e.g., 3c•4d), the open partially bound intermediate constitutes 42% of the 1:1 stoichiometry species. The most striking feature of the results in Table 5 is that the value of EM does not depend very strongly on the nature of the linkers. Table 5 includes an estimate of the total number of rotors connecting the two H-bonding sites (r), and although this varies from 5 to 20, the range of EM values is rather narrow (0.1–0.9 M).

DISCUSSION

The results in Table 5 allow us to explore the relationship between the structure of the linker groups, L1 and L2, and the effective molarity, EM, which quantifies the chelate cooperativity associated with formation of intramolecular H-bonds. Based on studies of EM values for the rates of covalent cyclization reactions, the two key parameters that are expected to affect

Table 5. Effective Molarities (M) Associated with Formation of the Intramolecular H-Bond in *c*-AA•DD Complexes at 298 K in CCl₄^a

complex	rotors (<i>r</i>)	EM (M)	¹ / ₂ KEM	population (%)	
				<i>c</i> -AA•DD	<i>o</i> -AA•DD
3a•4a	5	0.3	2.4	70	30
3a•4b	7	0.3	2.8	74	26
3a•4c	9	0.4	3.6	78	22
3a•4d	16	0.2	1.4	57	43
3b•4a	7	0.5	4.4	81	19
3b•4b	9	0.9	9.8	91	9
3b•4c	11	0.6	6.7	87	13
3b•4d	18	0.2	1.9	65	35
3c•4a	9	0.3	3.1	75	25
3c•4b	11	0.5	5.4	84	16
3c•4c	13	0.2	2.5	71	29
3c•4d	20	0.1	1.4	58	42

^aThe average error in EM is ±50%.

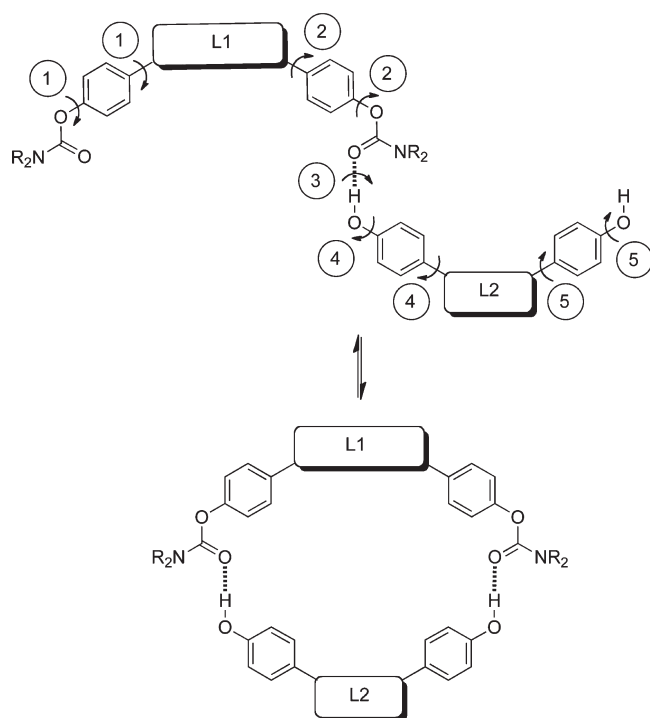


Figure 5. Approach used to count the number of rotors (*r*) that are conformationally restricted on formation of an intramolecular H-bond. When L1 and L2 are rigid, i.e., CH₂, there are five independent rotors which are labeled 1–5.

EM are ring strain and conformational flexibility.^{35,36} In the complexes described here, the inherent flexibility of the linker groups together with the relatively weak geometric constraints imposed by H-bonding should allow the formation of *c*-AA•DD complexes that are relatively strain-free, so we will focus on the conformational flexibility of the linker chains. Formation of an intramolecular H-bond leads to cyclization of the complex and restriction in the conformational mobility of the linkers. In

reality, it is the difference in conformational mobility between the free and bound states that we are interested in, but the crudest method for calibrating the system is simply to count rotors in the linkers.⁴⁷ Some assumptions must be applied in counting what is and is not a rotor, and the approach we have adopted is illustrated in Figure 5: the carbamate and the phenol OH groups are considered to have fixed conformations in conjugation with the aromatic rings; rotation around the aryl–oxygen bonds is equivalent to rotation around the aryl–carbon bonds, because spinning of the intermediate phenylene units does not affect the geometry of the complex; and the first intermolecular H-bond is considered to be a rotor (labeled 3 in Figure 5). For the 3a•4a complex, where both L1 and L2 are CH₂, there are only five rotors, as indicated in Figure 5. Increasing the length of the linkers increases the number of rotors (*r*) up to 20 as detailed in Table 5. This definition of *r* implies that the minimum value is *r* = 1, which is the rotor associated with the formation of the first intermolecular H-bond, labeled 3 in Figure 5.

Figure 6 shows the relationship between the number of rotors and EM for the complexes described in Table 5 (black dots). A clear trend is difficult to identify, but the results are more interesting when compared with data for other noncovalent cyclization processes. Figure 6 includes EM values for more rigid H-bonded complexes that we have reported previously, where *r* = 1 (Figure 7a,b, open circles in Figure 6),³¹ and data from the folding of sarcosine oligomers, where *r* is very large (*r* = 12–50) (Figure 7c, gray dots in Figure 6).⁴⁸ As might be expected, the more rigid complexes have higher EM values, and the very flexible systems have lower EMs. However, these results are particularly interesting when compared with the corresponding EM data for covalent cyclization reactions. Ring strain complicates the analysis of covalent cyclization processes, but Mandolini has collated literature data to estimate the EM for the rate of a strain-free covalent cyclization reaction as a function of the number of rotors in the linker.³⁵ This relationship is plotted as the gray line in Figure 6. For large numbers of rotors, the behavior of the covalent and noncovalent systems is practically identical. In this region, the relationship between log EM and log *r* is linear with a slope of –1.55. This is very close to the theoretical value of –1.5 that is expected for random walk encounters between end groups on a flexible chain.³⁸ However, as the number of rotors decreases, the very large EM values that are found for covalent cyclization of small rings are not observed for the noncovalent systems. Instead, the noncovalent EM values continue along the random walk line right up to the intersection with the log EM axis at EM ≈ 10 M. Thus, it appears that there is a relatively simple relationship between EM and the number of rotors (eq 9). This is consistent with the observations on ring–chain equilibria in supramolecular polymerization processes.⁴⁹

$$EM \approx 10r^{-3/2} \quad (9)$$

For systems of this type, where there is one rotational degree of freedom associated with formation of the first intermolecular H-bond (Figure 5), the maximum value of EM is on the order of 10 M, the intercept of 1.0 on the log EM axis in Figure 6. The value of EM is expected to be somewhat higher for perfectly rigid systems where there is no conformational mobility, and the Page and Jencks upper limit of 100 M is consistent with the data in Figure 6.³⁷

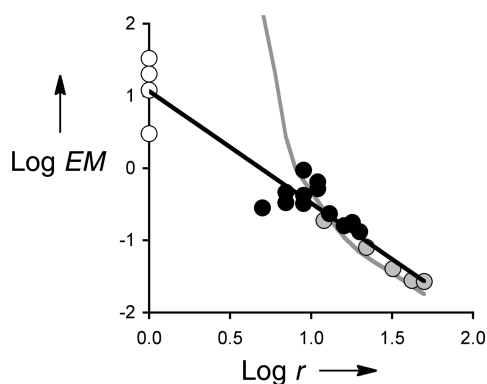


Figure 6. Relationship between the effective molarity (EM/M) at 298 K for covalent (gray line) and noncovalent (data points) cyclization processes and the number of rotors in the linking chain (r). The noncovalent EM values come from this work (black dots), related but more rigid H-bonded complexes (open circles) and folding of sarcosine oligomers (gray dots). The best fit straight line for the noncovalent data (black line) corresponds to $\log EM = 1.08 - 1.55 \log r$ ($r^2 = 0.91$).

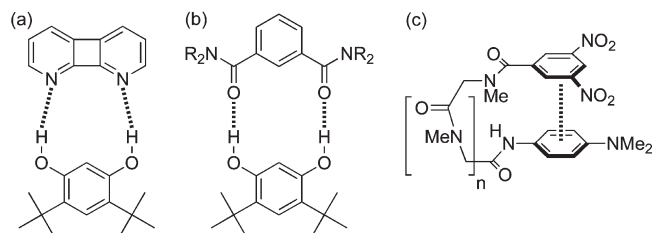


Figure 7. Experimental noncovalent EM data in Figure 6 is plotted (a, b) for H-bonded complexes with limited conformational mobility (open circles in Figure 6), and (c) for the folding of flexible sarcosine oligomers (gray dots in Figure 6).

CONCLUSIONS

We have developed a simple supramolecular model system for investigating the relationship between covalent structure and chelate cooperativity in the formation of intramolecular H-bonds. A chemical double mutant cycle analysis was used to confirm that the molecular design successfully avoids any complications due to secondary electrostatic interactions or allosteric cooperativity. However, there is a significant population partially bound states in some of the systems studied, and quantitative analysis of the titration experiments required consideration of partially bound complexes that contain only one H-bond, as well as fully bound 1:1 complexes that contain two H-bonds, and 2:1 complexes. Effective molarities (EMs) were measured for 12 different systems, where the number of rotors in the chains connecting the two H-bond sites was varied from 5 to 20. The association constants vary by less than an order of magnitude for all 12 complexes, and the variation in EM is remarkably small (0.1–0.9 M). The results were combined with data from the literature to come up with a general relationship for estimating the relationship between EM and the number of rotors in the connecting chains (r): $EM \approx 10r^{-3/2}$. The behavior is very different from that observed for covalent processes, where there is an increase in EM of several orders of magnitude for the cyclization of small rings, and the maximum value is on the order of 10^7 M.

Theory suggests that 100 M might represent an upper limit for the value of EM for a noncovalent intramolecular interaction.³⁷ The analysis presented here supports this idea, and indicates that introduction of rotors reduces the value of EM from this maximum in accord with a random walk analysis of the encounter probability of the chain ends. There are two important implications. Noncovalent EMs never reach the very high values observed for covalent processes, which places limitations on the magnitudes of the effects that one is likely to achieve through the use of chelate cooperativity in supramolecular assembly and catalysis. Second, the decrease in EM due to the introduction of conformational flexibility is less dramatic than one might expect on the basis of the behavior of covalent systems, which implies that the losses in binding affinity caused by poor preorganization are limited. Figure 6 shows that the EM falls by 2 orders of magnitude when the number of rotors is increased from 1 to 20. This implies that floppy design rather than preorganization could prove a fruitful strategy for supramolecular chemists. The EM does not fall below 0.1 M for any of the systems described here, and this means that the key chelate cooperativity parameter KEM will always be greater than 1, provided relatively high affinity interactions are used ($K_{\text{ref}} > 10 \text{ M}^{-1}$). Under these conditions, there will always be a thermodynamic benefit from chelate cooperativity, even for loosely linked multivalent systems.¹²

EXPERIMENTAL SECTION

Synthesis Compound 2a. A mixture of **1a** (0.579 g, 5.35 mmol), 4-nitrophenyl chloroformate (1.10 g, 5.35 mmol), and triethylamine (0.75 mL, 5.35 mmol) in dichloromethane (50 mL) was stirred under nitrogen atmosphere at room temperature for 4 days. Bis(2-ethylhexyl)amine (1.61 mL, 5.35 mmol) and triethylamine (0.75 mL, 5.35 mmol) were added, and the solution was stirred under nitrogen atmosphere at room temperature for an additional 5 days. The solution was diluted with dichloromethane (50 mL), washed with water (30 mL) and brine (30 mL), dried with sodium sulfate, and condensed under reduced pressure. The resulting oil was purified by column chromatography eluting with a dichloromethane and hexane. The product was isolated as a clear oil: yield 1.27 g (63%). $^1\text{H NMR}$ (250 MHz, CDCl_3) $\delta_{\text{H}} = 7.15$ (d, 2H, $J = 8$), 6.98 (d, 2H, $J = 8$), 3.28 (m, 4H), 2.34 (s, 3H), 1.75 (m, 2H), 1.35 (m, 16H), 0.92 (t, 12H, $J = 7$). $^{13}\text{C NMR}$ (62.8 MHz, CDCl_3) $\delta_{\text{C}} = 155.5, 149.4, 134.5, 129.7, 121.4, 51.1, 38.1, 37.4, 30.6, 28.7, 23.9, 23.1, 20.8, 14.1, 10.7$. MS (EI+) m/z (rel intens) = 268 (65), 375 (10) [M+]. HRMS (EI+) calcd for $\text{C}_{24}\text{H}_{41}\text{NO}_2$ 375.3134, found 375.3134. FT-IR (thin film) $\nu_{\text{max}}/\text{cm}^{-1}$ 2958, 2928, 2872, 1713, 1512, 1462, 1417, 1379, 1214, 1199.

Compound 2b. A mixture of **1b** (0.5 g, 2.5 mmol), 4-nitrophenyl chloroformate (0.5 g, 2.5 mmol), and triethylamine (0.35 mL, 2.5 mmol) in dry dichloromethane (50 mL) was stirred under nitrogen atmosphere at room temperature for 2 days. The solution was concentrated under reduced pressure. The crude product was dissolved in dichloromethane (15 mL), and bis(2-ethylhexyl)amine (0.97 mL, 2.7 mmol) and triethylamine (0.37 mL, 2.7 mmol) were added to the solution that was stirred overnight under nitrogen atmosphere at room temperature. The resulting slurry was dissolved in dichloromethane (50 mL), washed with hydrochloric acid 1 M (50 mL), sodium hydroxide 1 M (50 mL), water (50 mL), and brine (50 mL), dried with sodium sulfate, and then condensed under reduced pressure. The obtained oil was purified on silica eluting with a dichloromethane and hexane. The product was isolated as a clear oil: yield 0.3164 g (27%). $^1\text{H NMR}$ (250 MHz, CDCl_3) $\delta_{\text{H}} = 7.39$ (m, 5H), 6.98 (m, 4H), 5.06 (s, 2H), 3.27 (m, 4H), 1.75 (m, 2H), 1.34 (m, 16H), 0.92 (t, 12H, $J = 6$). $^{13}\text{C NMR}$ (62.9 MHz, CDCl_3) $\delta_{\text{C}} = 156.0, 155.6, 145.4, 128.6, 127.9$,

127.4, 122.5, 115.4, 70.5, 51.1, 50.9, 38.1, 37.4, 30.6, 28.7, 23.8, 23.1, 14.1, 10.7. MS (ES+) m/z (rel intens) = 468 (100) [M + H⁺], 485 (40), 490 (10) [M + Na⁺]. HRMS (ES+) calcd for C₃₀H₄₅NO₃Na 490.3297, found 490.3274. FT-IR (thin film) $\nu_{\max}/\text{cm}^{-1}$ 2957, 2928, 2859, 1714, 1507, 1463, 1418, 1379, 1194, 1152, 1104, 1025, 863, 819, 734, 696, 522.

Compound 3b⁵⁰. Compound **1b** (20.02 g, 99.98 mmol) was partially dissolved in dichloromethane (150 mL). To this solution were added solid potassium hydroxide (16.96 g, 302.26 mmol) and tetra-*N*-butylammonium bromide (3.83 g, 11.88 mmol). The mixture was stirred at room temperature for 40 h and then filtered over silica gel. Evaporation of the solvent gave a white solid (8.25 g, 20 mmol) that was dissolved in ethyl acetate (275 mL) and hydrogenated with palladium-on-charcoal (10% Pd, 0.4 g) and hydrogen gas at atmospheric pressure and room temperature. After removal of the catalyst via filtration, the solvent was evaporated and the resulting oil was recrystallized from ethyl acetate as a white solid: yield 4.24 g (91%). ¹H NMR (400 MHz, DMSO) δ_{H} = 9.09 (s, 2H), 6.88 (d, 4H, J = 8), 6.69 (d, 4H, J = 8), 5.57 (s, 2H). ¹³C NMR (62.8 MHz, DMSO) δ_{C} = 152.5, 149.2, 117.7, 115.7, 92.2. Mp = 121–123 °C. MS (ES–) m/z (rel intens) = 231 (100) [M – H⁺]. HRMS (ES–) calcd for C₁₃H₁₁O₄ 231.0657, found 231.0660. FT-IR (thin film) $\nu_{\max}/\text{cm}^{-1}$ 3393, 3034, 2040, 1867, 1609, 1503, 1452, 1407, 1365, 1317, 1241, 1196, 1169, 1145, 1111, 1100, 1038, 1003, 821, 809, 723, 639.

Compound 3c⁵¹. Compound **1b** (20.00 g, 99.90 mmol) was dissolved in acetone (125 mL). To this solution were added anhydrous potassium carbonate (20.50 g, 148.33 mmol) and 1,3-dibromopropane (5.07 mL, 49.90 mmol), and the mixture was refluxed for 3 days. The resulting solution was allowed to cool down and then filtered. The solvent was evaporated, and the crude product was dissolved in toluene (100 mL), washed with sodium hydroxide 1 M, and dried with sodium sulfate. Evaporation of the solvent gave a white solid, which was purified by recrystallization from acetone. After filtration, the crystals were dried (8.62 g, 19.57 mmol), dissolved in a mixture of tetrahydrofuran (220 mL) and methanol (58 mL), and hydrogenated with palladium-on-charcoal (10% Pd, 2 g) and hydrogen gas at atmospheric pressure and room temperature. After removal of the catalyst via filtration through celite, the solvent was evaporated and the product was crystallized from ethyl acetate as a yellow solid: yield 3.00 g (59%). ¹H NMR (400 MHz, DMSO) δ_{H} = 8.93 (s, 2H), 6.76 (d, 4H, J = 8), 6.66 (d, 4H, J = 8), 4.00 (t, 4H, J = 6), 2.07 (m, 2H). ¹³C NMR (62.9 MHz, DMSO) δ_{C} = 151.3, 151.2, 115.7, 115.4, 64.7, 28.9. Mp = 142–143 °C. MS (ES–) m/z (rel intens) = 259 (100) [M – H⁺]. HRMS (ES–) calcd for C₁₅H₁₅O₄ 259.0970, found 259.0980. FT-IR (thin film) $\nu_{\max}/\text{cm}^{-1}$ 3394, 3035, 2953, 2040, 1609, 1504, 1452, 1407, 1364, 1317, 1293, 1240, 1197, 1169, 1145, 1100, 1038, 995, 974, 820, 809, 724, 639.

Compound 3d⁵¹. Compound **1b** (13.34 g, 66.60 mmol) was dissolved in acetone (83.33 mL). To this solution were added anhydrous potassium carbonate (13.66 g, 98.87 mmol) and 1,10-dibromodecane (9.98 g, 33.26 mmol), and the mixture was refluxed for 3 days. The product precipitated as crystals that were washed with acetone, 1 M sodium hydroxide, and water (16.28 g, 30.24 mmol). After filtration, the crystals were dried (1 g, 1.86 mmol), partially dissolved in a mixture of chloroform and methanol (250 mL), and hydrogenated with palladium-on-charcoal (10% Pd, 0.23 g) and hydrogen gas at atmospheric pressure and room temperature. After removal of the catalyst via filtration through celite, the solvent was evaporated and the product was crystallized from a mixture of chloroform and methanol as a white solid: yield 0.22 g (33%). ¹H NMR (400 MHz, DMSO) δ_{H} = 8.88 (s, 2H), 6.72 (d, 4H, J = 9), 6.65 (d, 4H, J = 9), 3.83 (t, 4H, J = 6), 1.65 (m, 4H), 1.34 (m, 12H). ¹³C NMR (62.9 MHz, DMSO) δ_{C} = 151.5, 151.0, 115.7, 115.3, 67.9, 28.9, 28.8, 28.7, 25.5. Mp = 161–163 °C. MS (ES–) m/z (rel intens) = 357 (100) [M – H⁺]. HRMS (ES–) calcd for C₂₂H₂₉O₄ 357.2066, found 357.2070. FT-IR (thin film) $\nu_{\max}/\text{cm}^{-1}$ 3352, 3038,

2932, 2917, 2853, 1608, 1509, 1451, 1473, 1395, 1369, 1298, 1229, 1169, 1105, 1048, 1022, 983, 823, 802, 768, 556.

Compound 4a. A mixture of **3a** (0.620 g, 3.1 mmol), 4-nitrophenyl chloroformate (1.245 g, 6.2 mmol), and triethylamine (0.86 mL, 6.2 mmol) in dichloromethane (50 mL) was stirred under nitrogen atmosphere at room temperature for 48 h. Bis(2-ethylhexyl)amine (1.90 mL, 6.3 mmol) and triethylamine (0.86 mL, 6.2 mmol) were added, and the solution was stirred overnight under nitrogen atmosphere at room temperature. The solution was diluted with dichloromethane (50 mL), washed with water (30 mL) and brine (30 mL), dried with sodium sulfate, and condensed under reduced pressure. The resulting oil was purified by column chromatography eluting with a mixture of ethyl acetate and hexane. The product was isolated as a clear oil: yield 0.894 g (76.8%). ¹H NMR (250 MHz, CDCl₃) δ_{H} = 7.16 (d, 4H, J = 8), 7.01 (d, 4H, J = 8), 3.95 (s, 2H), 3.28 (m, 8H), 1.74 (m, 4H), 1.33 (m, 32H), 0.91 (m, 24H). ¹³C NMR (249.9 MHz, CDCl₃) δ_{C} = 155.4, 150.0, 137.7, 129.7, 121.6, 51.1, 50.9, 40.6, 38.1, 37.4, 30.6, 28.7, 23.9, 23.8, 23.1, 14.1, 10.7. MS (ES+) m/z (rel intens) = 736 (70) [M + H⁺], 758 (100) [M + Na⁺]. HRMS (ES+) calcd for C₄₇H₇₈N₂O₄Na 757.5859, found 757.5855. FT-IR (thin film) $\nu_{\max}/\text{cm}^{-1}$ 2957, 2927, 2859, 1717, 1508, 1464, 1417, 1379, 1198, 1165, 1053, 1018, 753, 508.

Compound 4b. A mixture of **3b** (6 g, 25.8 mmol), 4-nitrophenyl chloroformate (10.4 g, 51.6 mmol), and triethylamine (7.2 mL, 51.6 mmol) in dichloromethane (300 mL) was stirred under nitrogen atmosphere at room temperature for 48 h. Bis(2-ethylhexyl)amine (37.1 mL, 123.4 mmol) and triethylamine (14.4 mL, 103 mmol) were added, and the solution was stirred overnight under nitrogen atmosphere at room temperature. The solution was washed with 1 M hydrochloric acid, 1 M sodium hydroxide, water, and brine, dried with sodium sulfate, and condensed under reduced pressure. The resulting oil was purified by column chromatography eluting with a mixture of dichloromethane and hexane. The product was isolated as a clear oil: yield 4.0 g (20%). ¹H NMR (400 MHz, CDCl₃) δ_{H} = 7.09 (d, 4H, J = 8), 7.03 (d, 4H, J = 8), 5.67 (s, 2H), 3.25 (m, 8H), 1.75 (m, 4H), 1.35 (m, 32H), 0.92 (m, 24H). ¹³C NMR (100.6 MHz, CDCl₃) δ_{C} = 155.5, 154.1, 146.7, 122.6, 117.3, 92.1, 51.1, 50.9, 38.1, 37.4, 30.6, 28.7, 23.9, 23.8, 23.1, 14.1, 10.7. MS (ES+) m/z (rel intens) = 768 (80) [M + H⁺], 790 (100) [M + Na⁺], 806 (10) [M + K⁺]. HRMS (ES+) calcd for C₄₇H₇₉N₂O₆ 767.5938, found 767.5928. FT-IR (thin film) $\nu_{\max}/\text{cm}^{-1}$ 2957, 2927, 2859, 1717, 1505, 1464, 1418, 1379, 1185, 1139, 1014, 864, 818, 752, 521.

Compound 4c. A mixture of **3c** (4.6 g, 17.7 mmol), 4-nitrophenyl chloroformate (8.5 g, 42.2 mmol), and triethylamine (5.9 mL, 42.3 mmol) in dichloromethane (300 mL) was stirred under nitrogen atmosphere at room temperature for 48 h. Bis(2-ethylhexyl)amine (35.1 mL, 116.9 mmol) and triethylamine (16.3 mL, 116.9 mmol) were added, and the solution was stirred overnight under nitrogen atmosphere at room temperature. The solution was washed with 1 M hydrochloric acid, 1 M sodium hydroxide, water, and brine, dried with sodium sulfate, and condensed under reduced pressure. The resulting oil was purified by column chromatography eluting with dichloromethane and methanol. After removal of the solvent under reduced pressure, the product was isolated as a clear oil: yield 4.8 g (35%). ¹H NMR (250 MHz, CDCl₃) δ_{H} = 7.01 (d, 4H, J = 8), 6.89 (d, 4H, J = 8), 4.14 (t, 4H, J = 6), 3.27 (m, 8H), 2.25 (m, 2H), 1.74 (m, 4H), 1.34 (m, 32H), 0.92 (m, 24H). ¹³C NMR (62.9 MHz, CDCl₃) δ_{C} = 156.0, 155.6, 145.3, 122.5, 115.1, 65.0, 51.1, 37.4, 30.6, 29.3, 28.7, 23.9, 23.1, 14.1, 10.7. MS (ES+) m/z (rel intens) = 796 (30) [M + H⁺], 818 (100) [M + Na⁺], 834 (50) [M + K⁺]. HRMS (ES+) calcd for C₄₉H₈₃N₂O₆ 795.6251, found 795.6229. FT-IR (thin film) $\nu_{\max}/\text{cm}^{-1}$ 2957, 2927, 2859, 1715, 1507, 1464, 1418, 1379, 1294, 1193, 1141, 1105, 1060, 1010, 862, 819, 753, 520.

Compound 4d. A mixture of **3d** (1.0 g, 2.79 mmol), 4-nitrophenyl chloroformate (1.1 g, 5.56 mmol), and triethylamine (0.8 mL, 5.52

mmol) in dichloromethane (50 mL) was stirred under nitrogen atmosphere at room temperature for 48 h. Bis(2-ethylhexyl)amine (1.7 mL, 5.60 mmol) and triethylamine (0.8 mL, 5.52 mmol) were added, and the solution was stirred overnight under nitrogen atmosphere at room temperature. After evaporation of the solvent, the solution was diluted again with dichloromethane (50 mL), washed with water (30 mL) and brine (30 mL), dried with sodium sulfate, and condensed under reduced pressure. The resulting oil was purified on column chromatography eluting with ethyl acetate and hexane. The product was isolated as a clear oil: yield 0.8 g (32.1%). $^1\text{H NMR}$ (250 MHz, CDCl_3) $\delta_{\text{H}} = 7.00$ (d, 4H, $J = 8$), 6.87 (d, 4H, $J = 8$), 3.94 (t, 4H, $J = 6$), 3.28 (m, 8H), 1.76 (m, 8H), 1.32 (m, 44H), 0.92 (m, 24H). $^{13}\text{C NMR}$ (62.9 MHz, CDCl_3) $\delta_{\text{C}} = 156.3$, 155.7, 145.0, 122.4, 114.9, 68.4, 51.0, 50.8, 38.1, 37.4, 30.6, 29.5, 29.4, 29.3, 28.7, 26.0, 23.9, 23.8, 23.1, 14.1, 10.7. MS (ES+) m/z (rel intens) = 916 (100) $[\text{M} + \text{Na}^+]$. HRMS (ES+) calcd for $\text{C}_{56}\text{H}_{96}\text{N}_2\text{O}_6\text{Na}$ 915.7166, found 915.7164. FT-IR (thin film) $\nu_{\text{max}}/\text{cm}^{-1}$ 2956, 2926, 2857, 1717, 1508, 1464, 1418, 1380, 1295, 1197, 1152, 1104, 861, 818, 753, 521.

$^1\text{H NMR}$ Titrations. A 10 mL sample of host dissolved in CCl_4 was prepared at known concentration (0.1–0.6 mM). A 0.6 mL fraction of this solution was used to record a $^1\text{H NMR}$ spectrum using a capillary of D_2O as a lock signal. The host stock solution was used to prepare a 2 mL solution of guest at known concentration (40–400 mM), so that the concentration of the host remained constant throughout the titration. Aliquots of the guest solution were successively added to the NMR tube containing the host solution, and a $^1\text{H NMR}$ spectrum was recorded after each addition. Changes in chemical shift for the host aromatic and phenolic protons signals were fit to 1:1 and 2:1 binding isotherms using purpose written software. Each titration was repeated at least twice, and the error is quoted as twice the standard deviation.

■ ASSOCIATED CONTENT

S Supporting Information. Calculation of EM for the folding of sarcosine oligomers at 298 K. Comparison of the quality of fit of the titration data to 1:1 and 2:1 isotherms. NMR data for all compounds. This material is available free of charge via the Internet at <http://pubs.acs.org>.

■ AUTHOR INFORMATION

Corresponding Author
c.hunter@sheffield.ac.uk

Notes

Phone: +44 (0)114 2229476. Fax: +44 (0)114 2229436.

■ ACKNOWLEDGMENT

We thank the EPSRC for funding.

■ REFERENCES

- Lehn, J.-M. *Angew. Chem., Int. Ed.* **1990**, *29*, 1304–1319.
- Prins, L. J.; Reinhoudt, D. N.; Timmerman, P. *Angew. Chem., Int. Ed.* **2001**, *40*, 2382–2426.
- Mulder, A.; Huskens, J.; Reinhoudt, D. N. *Org. Biomol. Chem.* **2004**, *2*, 3409–3424.
- Badjic, J. D.; Nelson, A.; Cantrill, S. J.; Turnbull, W. B.; Stoddart, J. F. *Acc. Chem. Res.* **2005**, *38*, 723–732.
- Hughes, A. D.; Anslyn, E. V. *Proc. Natl. Acad. Sci. U. S. A.* **2007**, *104*, 6538–6543.
- Mammen, M.; Choi, S. K.; Whitesides, G. M. *Angew. Chem., Int. Ed.* **1998**, *37*, 2755–2794.
- Ercolani, G. *J. Am. Chem. Soc.* **2003**, *125*, 16097–16103.
- Hunter, C. A.; Anderson, H. L. *Angew. Chem., Int. Ed.* **2009**, *48*, 7488–7499.
- Herskovits, T. T. *Biochemistry* **1963**, *2*, 335–340.
- Pörschke, D. *Biopolymers* **1971**, *10*, 1989–2013.
- Crothers, D. M.; Metzger, H. *Immunochemistry* **1972**, *9*, 341–357.
- Kitov, P. I.; Sadowska, J. M.; Mulvey, G.; Armstrong, G. D.; Ling, H.; Pannu, N. S.; Read, R. J.; Bundle, D. R. *Nature* **2000**, *403*, 669–672.
- Badjic, J. D.; Balzani, V.; Credi, A.; Silvi, S.; Stoddart, J. F. *Science* **2004**, *303*, 1845–1849.
- Fang, L.; Olson, M. A.; Benitez, D.; Tkatchouk, E.; Goddard, W. A.; Stoddart, J. F. *Chem. Soc. Rev.* **2010**, *39*, 17–29.
- Ludden, M. J. W.; Reinhoudt, D. N.; Huskens, J. *Chem. Soc. Rev.* **2006**, *35*, 1122–1134.
- Philp, D.; Stoddart, J. F. *Angew. Chem., Int. Ed.* **1996**, *35*, 1155–1196.
- Huskens, J.; Mulder, A.; Auletta, T.; Nijhuis, C. A.; Ludden, M. J. W.; Reinhoudt, D. N. *J. Am. Chem. Soc.* **2004**, *126*, 6784–6797.
- Ten Cate, A. T.; Kooijman, H.; Spek, A. L.; Sijbesma, R. P.; Meijer, E. W. *J. Am. Chem. Soc.* **2004**, *126*, 3801–3808.
- De Greef, T. F. A.; Nieuwenhuizen, M. M. L.; Sijbesma, R. P.; Meijer, E. W. *J. Org. Chem.* **2010**, *75*, 598–610.
- Rao, J.; Lahiri, J.; Isaacs, L.; Weis, R. M.; Whitesides, G. M. *Science* **1998**, *280*, 708–711.
- Krishnamurthy, V. M.; Semetey, V.; Bracher, P. J.; Shen, N.; Whitesides, G. M. *J. Am. Chem. Soc.* **2007**, *129*, 1312–1320.
- Cockroft, S. L.; Hunter, C. A. *Chem. Soc. Rev.* **2007**, *36*, 172–188.
- Abraham, M. H.; Platts, J. A. *J. Org. Chem.* **2001**, *66*, 3484–3491.
- Hunter, C. A. *Angew. Chem., Int. Ed.* **2004**, *43*, 5310–5324.
- Calderone, C. T.; Williams, D. H. *J. Am. Chem. Soc.* **2001**, *123*, 6262–6267.
- Shinkai, S.; Ikeda, M.; Sugasaki, A.; Takeuchi, M. *Acc. Chem. Res.* **2001**, *34*, 494–503.
- Tobey, S. L.; Anslyn, E. V. *J. Am. Chem. Soc.* **2003**, *125*, 10963–10970.
- Williams, D. H.; Davies, N. L.; Zerella, R.; Bardsley, B. *J. Am. Chem. Soc.* **2004**, *126*, 2042–2049.
- Williams, D. H.; Stephens, E.; O'Brien, D. P.; Zhou, M. *Angew. Chem., Int. Ed.* **2004**, *43*, 6596–6616.
- Chekmeneva, E.; Hunter, C. A.; Packer, M. J.; Turega, S. M. *J. Am. Chem. Soc.* **2008**, *130*, 17718–17725.
- Camara-Campos, A.; Musumeci, D.; Hunter, C. A.; Turega, S. *J. Am. Chem. Soc.* **2009**, *131*, 18518–18524.
- Hunter, C. A.; Ihekwaba, N.; Misuraca, M. C.; Segarra-Maset, M. D.; Turega, S. M. *Chem. Commun.* **2009**, 3964–3966.
- Camara-Campos, A.; Hunter, C. A.; Tomas, S. *Proc. Natl. Acad. Sci. U. S. A.* **2006**, *103*, 3034–3038.
- Schneider, H.-J. *Angew. Chem., Int. Ed.* **2009**, *48*, 2–56.
- Galli, C.; Mandolini, L. *Eur. J. Org. Chem.* **2000**, 3117–3125.
- Kirby, A. *Adv. Phys. Org. Chem.* **1980**, *17*, 183.
- Page, M. I.; Jencks, W. P. *Proc. Natl. Acad. Sci. U. S. A.* **1971**, *68*, 1678–1683.
- Kuhn, W. *Kolloidn. Zh.* **1934**, *68*, 2–15.
- Andrews, P. R.; Craik, D. J.; Martin, J. L. *J. Med. Chem.* **1984**, *27*, 1648–1657.
- Zimmerman, S. C.; Mrksich, M.; Baloga, M. *J. Am. Chem. Soc.* **1989**, *111*, 8528–8530.
- Searle, M. S.; Williams, D. H. *J. Am. Chem. Soc.* **1992**, *114*, 10690–10697.
- Searle, M. S.; Williams, D. H.; Gerhard, U. *J. Am. Chem. Soc.* **1992**, *114*, 10697–10704.
- Bohm, H. J. *J. Comput.-Aided Mol. Des.* **1994**, *8*, 243–256.
- Hossain, M. A.; Schneider, H.-J. *Chem.—Eur. J.* **1999**, *5*, 1284–1290.
- Corbin, P. S.; Zimmerman, S. C.; Thiessen, P. A.; Hawryluk, N. A.; Murray, T. J. *J. Am. Chem. Soc.* **2001**, *123*, 10475–10488.

(46) Quinn, J. R.; Zimmerman, S. C.; Del Bene, J. E.; Shavitt, I. *J. Am. Chem. Soc.* **2007**, *129*, 934–941.

(47) Cacciapaglia, R. C.; Di Stefano, S.; Mandolini, L. *Acc. Chem. Res.* **2004**, *37*, 113–122.

(48) Sisido, M.; Takagi, H.; Imanishi, Y.; Higashimura, T. *Macromolecules* **1977**, *10*, 125–130.

(49) De Greef, T. F. A.; Smulders, M. M. J.; Wolfs, M.; Schenning, A. P. H. J.; Sijbesma, R. P.; Meijer, E. W. *Chem. Rev.* **2009**, *109*, 5687–5754.

(50) Hopf, H.; Utermöhlen, R.; Jones, P. G.; Desvergne, J.-P.; Bouas-Laurent, H. *J. Org. Chem.* **1992**, *57*, 5509–5517.

(51) Kierstead, R. W.; Faraone, A.; Mennona, F.; Mullin, J.; Guthrie, R. W.; Crowley, H.; Simko, B.; Blaber, L. C. *J. Med. Chem.* **1983**, *26*, 1561–1569.